

## Thermochemistry of stuffed quartz-derivative phases along the join $\text{LiAlSiO}_4\text{-SiO}_2$

HONGWU XU,<sup>1,\*</sup> PETER J. HEANEY,<sup>1,†</sup> ALEXANDRA NAVROTSKY,<sup>1,‡</sup> LETITIA TOPOR,<sup>1</sup> AND JUN LIU<sup>2</sup>

<sup>1</sup>Department of Geosciences and Princeton Materials Institute, Princeton University, Princeton, New Jersey 08544, U.S.A.

<sup>2</sup>Center for High Pressure Research and Department of Geosciences,  
State University of New York at Stony Brook, Stony Brook, New York 11794, U.S.A.

### ABSTRACT

Enthalpies of drop-solution ( $\Delta H_{\text{drop-soln}}$ ) of a suite of stuffed quartz-derivative phases with the composition  $\text{Li}_{1-x}\text{Al}_{1-x}\text{Si}_{1+x}\text{O}_4$  ( $0 \leq x \leq 1$ ) have been measured in molten  $2\text{PbO}\cdot\text{B}_2\text{O}_3$  at 974 K. Substitution of  $\text{Si}^{4+}$  for  $\text{Li}^+\text{+Al}^{3+}$  results in more exothermic enthalpies of drop-solution, which is consistent with behavior seen in other crystalline and glassy aluminosilicates. Al/Si ordering serves to stabilize these phases, and long-range ordering for compositions with  $x$  approximately  $<0.3$  can be discerned in both calorimetric data and in structural data obtained by electron and synchrotron X-ray diffraction (XRD). In contrast, a structural but not an energetic discontinuity is apparent at  $x \cong 0.65$ , which corresponds to a compositionally induced  $\alpha$ - $\beta$  quartz transition with a small enthalpy of transformation.

An enthalpy for the Al/Si order-disorder reaction in  $\beta$ -eucryptite was measured as  $25.9 \pm 2.6$  kJ/mol. Standard molar enthalpies of formation of the stuffed quartz-derivative phases from constituent oxides ( $\Delta H_{\text{f,ox}}^0$ ) and elements ( $\Delta H_{\text{f,el}}^0$ ) at 298 K also are presented.  $\Delta H_{\text{f,ox}}^0 = -69.78 \pm 1.38$  kJ/mol and  $\Delta H_{\text{f,el}}^0 = -2117.84 \pm 2.50$  kJ/mol for  $\beta$ -eucryptite, which are in good agreement with results previously determined by HF solution calorimetry at 346.7 K (Barany and Adami 1966). The enthalpies of formation of other compositions are reported for the first time.

### INTRODUCTION

$\text{Li}_{1-x}\text{Al}_{1-x}\text{Si}_{1+x}\text{O}_4$  aluminosilicates ( $0 \leq x \leq 1$ ), which crystallize in either the  $\beta$ - or  $\alpha$ -quartz structure, are of considerable interest for their unique physical properties and for the insight they provide into general crystal-chemical systematics (Palmer 1994). The end-member  $\beta$ -eucryptite ( $\text{LiAlSiO}_4$ ) has one-dimensional superionic conductivity (Alpen et al. 1977; Nagel and Böhm 1982), and hence it potentially can be used as a solid electrolyte in lithium-based batteries. Intermediate compositions are common components of high-temperature glass-ceramic products due to their near-zero thermal expansion and appropriate viscosity for high-speed glass-forming (Beall 1994).

In addition, the  $\text{LiAlSiO}_4\text{-SiO}_2$  join offers an ideal system for investigations of Al/Si order-disorder behavior. In many mineral groups, such as feldspars, Al/Si ordering is accompanied by other phase transitions and by complex subsolidus phenomena such as exsolution (e.g., Ribbe 1983). These complementary reactions can make it very difficult to isolate the effects that Al/Si ordering exerts on mineral thermochemistry. By contrast, stuffed quartz-derivative phases along the  $\text{LiAlSiO}_4\text{-SiO}_2$  join are relatively simple in structure, and thus

they offer a better solid-solution series for studying Al/Si ordering.

The structure of quartz consists of paired chains of silica tetrahedra that spiral in left- or right-handed helices about the  $c$ -axis (e.g., Heaney and Veblen 1991). In  $\beta$ -quartz, these chains obey an apparent sixfold screw symmetry, and they produce open channels parallel to  $c$ . When  $\beta$ -quartz is cooled below 846 K at 1 bar, however, the expanded  $\beta$ -quartz framework collapses displacively to the denser  $\alpha$ -quartz configuration, involving a space group change from  $P6_222$  or  $P6_422$  to  $P3_121$  or  $P3_121$ .

While pure  $\beta$ -quartz is not quenchable, the incorporation of certain small cations (such as  $\text{Li}^+$ ,  $\text{Mg}^{2+}$ , and  $\text{Zn}^{2+}$ ) into the structural channels can prop open the framework and stabilize the structure of  $\beta$ -quartz at room temperature (Beall 1994). Charge balance may be achieved by replacing a fraction of the  $\text{Si}^{4+}$  ions by  $\text{Al}^{3+}$ . In the  $\text{LiAlSiO}_4\text{-SiO}_2$  system, the  $\beta$ -quartz structure persists to room temperature for compositions below  $x \cong 0.67$  (Beall 1994; Xu et al. in review). As expected, the more siliceous compositions adopt the  $\alpha$ -quartz modification.

Crystal structure analyses of the end-member  $\beta$ -eucryptite have revealed that its translational periodicity is doubled along  $c$  and  $a$  relative to  $\beta$ -quartz (Winkler 1948; Buerger 1954; Schulz and Tscherry 1972a, 1972b; Tscherry et al. 1972a, 1972b; Pillars and Peacor 1973; Lichtenstein et al. 1998; Xu et al. 1999a, 1999b). This superstructure arises from the ordering of Al and Si ions in alternate layers normal to  $c$  with concomitant ordering of Li within two distinct channels. However, with increasing silica content for the  $\text{Li}_{1-x}\text{Al}_{1-x}\text{Si}_{1+x}\text{O}_4$  phases at room temperature, the superstructure is gradually lost and dis-

\*E-mail: hxu@ucdavis.edu

†Present address: Thermochemistry Facility, Department of Chemical Engineering and Materials Science, University of California at Davis, Davis, California 95616, U.S.A.

‡Present address: Department of Geosciences, The Pennsylvania State University, University Park, Pennsylvania 16802, U.S.A.

appears at  $x \approx 0.3$  (Xu et al. in review), which suggests an Al/Si order-disorder transition at this composition.

Several phase-equilibrium studies in the  $\text{Li}_2\text{O}-\text{Al}_2\text{O}_3-\text{SiO}_2$  (LAS) system have demonstrated that members of the  $\beta$ -eucryptite- $\alpha$ -quartz series display different thermodynamic behaviors at atmospheric pressure (e.g., Hatch 1943; Roy and Osborn 1949; Beall et al. 1967; Strnad 1986). The compounds near  $\beta$ -eucryptite in composition ( $x = 0 - \sim 0.22$ ) are stable at high temperature (Fig. 1). For example,  $\beta$ -eucryptite is stable from its melting point ( $\sim 1673$  K) to  $\sim 1245$  K, at which temperature it reconstructively transforms to  $\alpha$ -eucryptite (Roy et al. 1950; Hummel 1952). However, more silicic stuffed quartz-derivative phases are metastable at all temperatures. Upon prolonged heating at high temperature ( $>1173$  K), these phases tend either to transform to keatite solid solutions (s.s.) or to decompose into keatite solid solutions and  $\alpha$ -cristobalite, depending on their silica content (Beall 1994) (Fig. 1).

In contrast, the high-pressure behavior of this system has received much less attention. The only high-pressure phase-equilibrium relation study (Munoz 1969) reveals that the  $\beta$ -quartz stuffed-derivative phase with the composition  $\text{LiAlSi}_2\text{O}_6$  ( $x \approx 0.33$ ) is stable over a pressure range of 10–26.5 kbar at high temperature. The study of Munoz (1969) also suggests that the silica-rich compositions ( $x > 0.33$ ), which are metastable at 1 atm, may have stability regions above 10 kbar.

Although extensive phase-equilibrium studies have been performed for this system, only a few calorimetric investigations of the stuffed quartz-derivative compounds have been undertaken, and they have focused on the end-member  $\beta$ -eucryptite (Barany and Adami 1966) and on glass (Roy and Navrotsky 1984). Thus, the energetic systematics of this solid-solutions series remain largely undetermined. In addition, enthalpies of formation of the intermediate phases have not been reported. High-temperature solution calorimetry has proven to be a successful technique for studying the thermodynamics and kinetics of solid solutions and order-disorder reactions in many systems (Navrotsky 1997), including framework silicates such as feldspars (Carpenter et al. 1985; Carpenter 1991; Hovis and Navrotsky 1995) and cordierite (Carpenter et al. 1983). The purpose of this work is to determine the thermochemical pa-

rameters of stuffed quartz-derivative solid solutions along the  $\text{LiAlSiO}_4-\text{SiO}_2$  join by high-temperature solution calorimetry and to relate them to their crystal chemistry.

## EXPERIMENTAL METHODS

### Sample preparation

Stuffed quartz-derivative phases with the composition  $\text{Li}_{1-x}\text{Al}_{1-x}\text{Si}_{1+x}\text{O}_4$ ,  $x = 0, 0.2, 0.25, 0.33, 0.5, 0.69, 0.7,$  and  $0.9$ , were used in this study. Because these phases exhibit different thermodynamic stability regions or are even metastable, three synthesis methods were employed: high-temperature sintering, high-pressure synthesis, and glass annealing.

As  $\text{LiAlSiO}_4$  and  $\text{Li}_{0.8}\text{Al}_{0.8}\text{Si}_{1.2}\text{O}_4$  are stable phases between  $\sim 1273$  and  $\sim 1673$  K at atmospheric pressure, they can readily be prepared by conventional high-temperature sintering. Stoichiometric amounts of  $\text{Li}_2\text{CO}_3$  (Aesar 99.999%, dried at 398 K prior to use),  $\text{Al}_2\text{O}_3$  (Aesar 99.99%, annealed at 1773 K prior to use), and  $\text{SiO}_2 \cdot n\text{H}_2\text{O}$  (Fisher) powders were ground and mixed in an agate mortar and heated in a platinum crucible at 1373 K for 15 h. The resulting products were then well ground and annealed at 1573 K for 24 h.

However, the high-temperature sintering method yielded stuffed keatite-derivative phases for starting stoichiometries of  $x = 0.25, 0.33,$  and  $0.5$ , and mixtures of stuffed keatite-derivative phases and  $\alpha$ -cristobalite for  $x = 0.7$  and  $0.9$ . Therefore, the stuffed quartz-derivative phases of these compositions were synthesized by either high-pressure high-temperature processing or by glass annealing.

The experimental conditions and starting materials for high- $P$  and high- $T$  syntheses are listed in Table 1. Preparation of the  $x = 0.33$  phase was performed in a PC3 high- $P$  and high- $T$  tabletop piston-cylinder apparatus (Depths of the Earth Co.). The starting material was  $\sim 70$  mg of  $\beta$ -spodumene, which has the keatite structure and was obtained by high- $T$  processing of the oxides. This material was packed into a platinum capsule, whose length was half that of the graphite furnace after both ends were sealed ( $\sim 1.5$  cm). The platinum capsule was then placed into a heat-treated pyrophyllite cup, surrounded by the graphite furnace. The furnace was separated from the NaCl outer bushing by a pyrex glass sleeve. A W3%Re/W25%Re thermocouple and a digital Eurotherm 818 controller were used to control temperature. At the start of the experiment, temperature and pressure were increased simultaneously until 1473 K and 15 kbar. The annealing time at these conditions was about 2 h. At the end of the experiment, the sample assembly was quenched down to room temperature, and then the pressure was released slowly.

The phases with  $x = 0.5, 0.7,$  and  $0.9$  were prepared using a

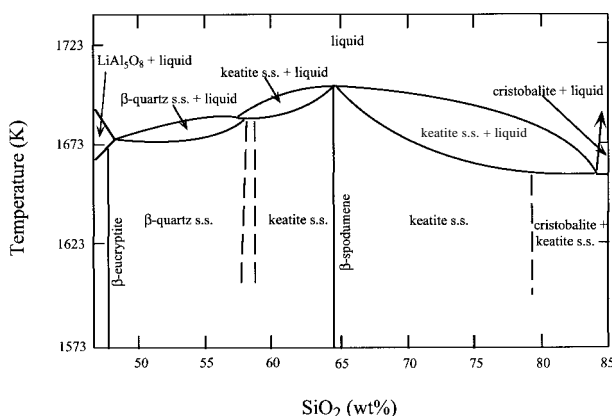


FIGURE 1. Phase diagram of the  $\text{Li}_{1-x}\text{Al}_{1-x}\text{Si}_{1+x}\text{O}_4$  system (After Strnad 1986 and Beall 1994).

TABLE 1. Experimental conditions and starting materials for the high-pressure syntheses of the stuffed quartz-derivative phases  $\text{Li}_{1-x}\text{Al}_{1-x}\text{Si}_{1+x}\text{O}_4$

$x$	$P$ (kbar)	$T$ (K)	$t$ (h)	starting material
0.33	15	1473	2	keatite s.s.
0.5	20	1488	2	keatite s.s.
0.7	20	1513	1.5	keatite s.s. + $\alpha$ -cristobalite
0.9	20	1513	2	keatite s.s. + $\alpha$ -cristobalite

Note: s.s. = solid solutions.

girdle press in the High-Pressure Synthesis Laboratory at Stony Brook. The sample assembly is very similar to the one described above, except that an MgO sleeve rather than NaCl was used. In addition, temperatures were determined based on a previously calibrated power-temperature relationship.

The stuffed quartz-derivative samples with  $x = 0.25$  and  $0.69$  were crystallized from glasses of corresponding compositions at 1023 K for 7 h and 1123 K for 4 h, respectively. The glasses were made by melting stoichiometric amounts of  $\text{Li}_2\text{CO}_3$ ,  $\text{Al}_2\text{O}_3$ , and  $\text{SiO}_2 \cdot n\text{H}_2\text{O}$  powders in a platinum crucible at 1873 K for  $\sim 8$  h and then quenching in air, and they were ground into powders of about 10  $\mu\text{m}$  size before being heat-treated in a muffle furnace. In addition, a series of  $\beta$ -eucryptite samples were prepared by the same method. The crystallization temperature ranged from 1073 to 1523 K and the annealing time from 1 to 70.5 h (see Table 2 for details).

### Sample characterization

**Electron microprobe analysis.** The compositions of the synthesized samples were determined by electron probe microanalysis using a Cameca SX-50 instrument at Princeton University operated at 15 kV accelerating potential and with a beam current of 20 nA. The  $\text{Al}_2\text{O}_3$  and  $\text{SiO}_2$  contents of the samples were analyzed with kyanite as the calibration standard. Because the X-ray emission from Li cannot be detected with the electron microprobe, and because no other elements were detected in the samples, the  $\text{Li}_2\text{O}$  content was calculated by difference assuming  $\text{Li}_2\text{O}\% + \text{Al}_2\text{O}_3\% + \text{SiO}_2\% = 100\%$ . The analyses showed that compositions agreed well with their nominal values (by  $<2$  wt% difference) and that the samples were homogeneous.

**Synchrotron X-ray diffraction.** Powder XRD measurements were carried out with a linear position-sensitive detector (PSD) at beam line X7A (Cox et al. 1988) of the National Synchrotron Light Source (NSLS), Brookhaven National Laboratory (BNL). The wavelengths used were 0.700789  $\text{\AA}$  (for  $x = 0$  and  $0.2$ ), 0.790012  $\text{\AA}$  (for  $x = 0.5$ ), and 0.799316  $\text{\AA}$  (for  $x = 0.33, 0.69, 0.7$ , and  $0.9$ ), as calibrated using a  $\text{CeO}_2$  standard. The powder samples were sealed in 0.02 mm diameter quartz-glass capillaries, and the capillaries were either fully rotated or rocked  $\pm 10^\circ$  during data collection. Data were collected from  $7^\circ$  to  $60^\circ$   $2\theta$  in step scan mode using steps of  $0.25^\circ$  with counting times of 10 s ( $7$ – $20^\circ$ ), 20 s ( $20$ – $35^\circ$ ), 40 s ( $35$ – $50^\circ$ ), and 80 s ( $50$ – $60^\circ$ ) per step.

Rietveld refinements were performed using the general

structure analysis system (GSAS) program of Larson and Von Dreele (1994). The starting atomic parameters for the phases with  $x = 0$  and  $0.2$  were obtained from the study of  $\beta$ -eucryptite by Guth and Heger (1979), and those for other compositions from the study of the  $\text{LiAlSi}_2\text{O}_6$  stuffed quartz-derivative phase by Li (1968). Parameters were refined as follows: after scale factor and four RDF (radial distribution function) background terms had converged, specimen displacement and lattice parameters were added and optimized. Between two and twelve additional background terms were then added, and the peak profiles were fitted mainly by refining the Lorentzian components in a pseudo-Voigt function (Thompson et al. 1982). Finally, the atomic positions and temperature factors of Li, Al, Si, and O were refined, yielding  $R_{\text{wp}}$  values ranging from 4.5% to 6.9%. Details of the full structural refinements are presented by Xu et al. (in review).

**Electron diffraction.** Specimens for TEM experiments were prepared by grinding each of the synthesized samples in an agate mortar and placing a drop of sample-alcohol suspension on a holey-carbon grid. Electron diffraction was performed with a Philips FEG CM-200 microscope equipped with a supertwin objective lens and operated at 200 keV.

### High-temperature calorimetry

All high-temperature calorimetric measurements were performed using a Tian-Calvet microcalorimeter operating at  $974 \pm 1$  K, described in detail elsewhere (Navrotsky 1997). Two types of experiments were conducted: (1) Drop-solution calorimetry was done with molten lead borate ( $2\text{PbO} \cdot \text{B}_2\text{O}_3$ ) solvent. A sample pellet weighing  $\sim 5$  mg (for high- $P$  samples) or  $\sim 15$  mg (for high- $T$  sintering and glass-annealing samples) was dropped from room temperature into the molten lead borate solvent in the calorimeter at 974 K. The enthalpy of drop solution includes the energy associated with heating the sample from room temperature to the calorimeter temperature plus the enthalpy of solution of the sample. (2) Transposed temperature drop calorimetry involves experiments in which the sample pellet was dropped from room temperature into the calorimeter at 974 K, without the presence of solvent. The measured heat effect corresponds to the heat content, ( $H_{974} - H_{298}$ ), of the sample. The difference between the enthalpy of drop-solution and heat content of a sample yields its enthalpy of solution. A drop-solution experiment for  $\text{Li}_2\text{CO}_3$  was carried out under a flowing argon atmosphere with a flow rate of  $\sim 90$   $\text{cm}^3/\text{min}$  to sweep out the evolved  $\text{CO}_2$  (Navrotsky et al. 1994). This measurement provided reference data for  $\text{Li}_2\text{O}$  for the enthalpy of formation calculations. All other experiments were performed in static air.

## RESULTS

### Dependence of symmetry and unit-cell parameters on Li+Al content

In  $\beta$ -eucryptite, two types of superlattice reflections are produced by atomic ordering: (1)  $c$ -reflections ( $h, k = \text{even}; l = \text{odd}$ ), which result from Al/Si configurational order; and (2)  $a$ -reflections ( $h, k = \text{odd}$  or  $h+k = \text{odd}; l = \text{odd}$ ), which indicate Li positional order (Tscherry et al. 1972b; Müller and Schulz 1976; Xu et al. 1999a).

**TABLE 2.** Enthalpies of drop solution in lead borate at 974 K of  $\beta$ -eucryptite ( $\text{LiAlSiO}_4$ ) samples synthesized by annealing glasses at various temperatures and times

$T$ (K)	$t$ (h)	$\Delta H_{\text{drop-soln},974}$ (kJ/mol)*
1073	1	138.11 $\pm$ 0.31(4)
1073	5.25	138.80 $\pm$ 1.11(5)
1173	1	139.55 $\pm$ 1.91(5)
1173	5.25	143.73 $\pm$ 1.52(5)
1173	16.7	147.30 $\pm$ 1.92(6)
1173	70.5	152.72 $\pm$ 1.20(4)
1323	5.25	153.72 $\pm$ 1.93(6)
1523	33	153.08 $\pm$ 1.89(5)

\*Uncertainty is two standard deviations of mean; value in parentheses is the number of experiments.

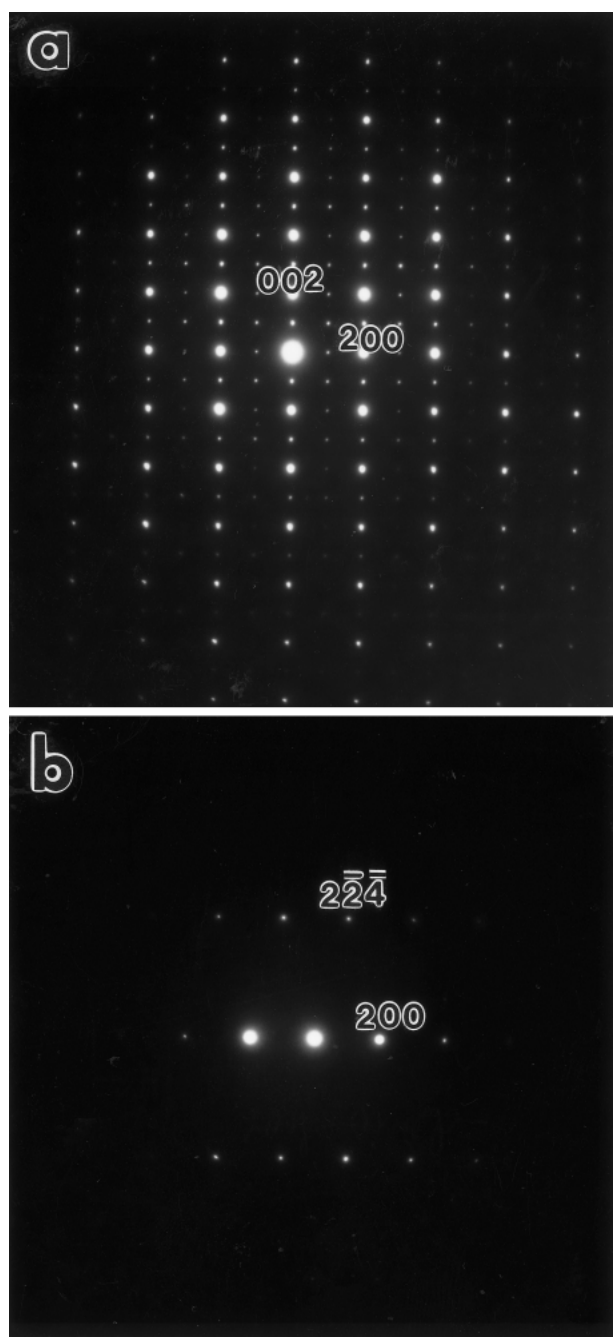


**FIGURE 2.** SAED patterns of the stuffed quartz-derivative phases  $\text{Li}_{1-x}\text{Al}_{1-x}\text{Si}_{1+x}\text{O}_4$ . (a)  $x = 0$ ; (b)  $x = 0.69$ . The patterns are indexed in terms of the  $\beta$ -eucryptite unit-cell.

Figure 2a is a [010] selected-area electron diffraction (SAED) pattern of  $\beta$ -eucryptite. As seen in this figure, both  $c$ - and  $a$ -reflections are evident, confirming Al/Si ordering and Li positional ordering in our sample. Our synchrotron XRD patterns of the same sample also exhibited such  $c$ -reflection peaks as 201 and 003 (Fig. 3a), although the patterns failed to reveal  $a$ -reflections due to the small scattering factor for Li. However, for silica-rich members of the series ( $x \geq 0.33$ ), neither  $c$ - nor  $a$ -reflections

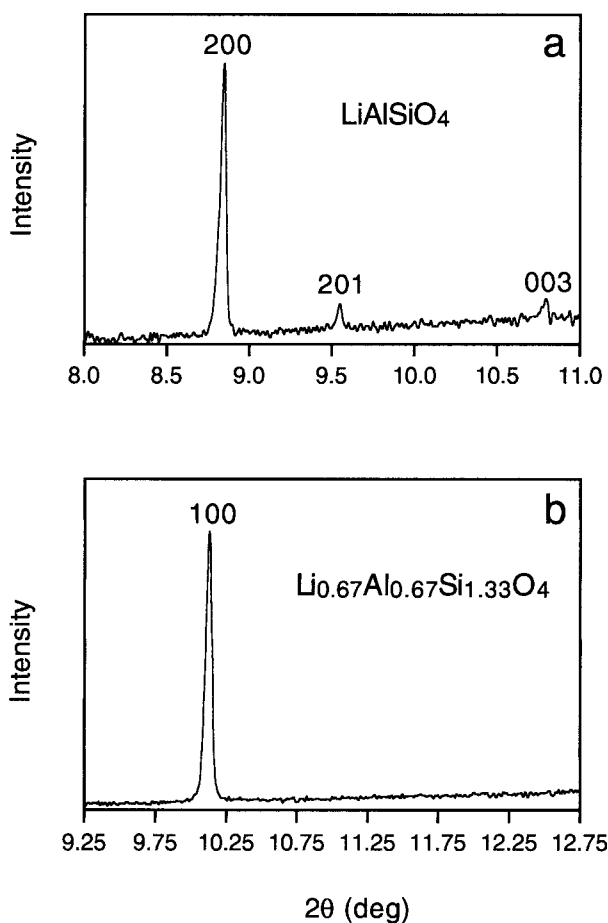


**FIGURE 3.** Synchrotron XRD patterns for the  $\text{Li}_{1-x}\text{Al}_{1-x}\text{Si}_{1+x}\text{O}_4$  phases with (a)  $x = 0$  and (b)  $x = 0.33$ . Note that the superlattice peaks 201 and 003 are present in pattern a but absent in b. Pattern a is indexed in terms of the superstructure cell, and pattern b is based on the basic quartz-like cell.

could be discerned by electron diffraction (Fig. 2b) and synchrotron XRD (Fig. 3b), indicating that long-range Al/Si configurational order and Li positional order are absent in structures with these compositions.

The unit-cell dimensions of the ordered structure ( $a_o$ ,  $c_o$ ) are related to those of the disordered phase ( $a_d$ ,  $c_d$ ) by  $a_o = 2a_d$  and  $c_o = 2c_d$ . Table 3 and Figure 4 shows the dependence of unit-cell dimensions on Li+Al substitution for Si in terms of the disordered cell (Xu et al. in review); the cell parameters for the ordered phases are plotted as  $a'_o = a_o/2$  and  $c'_o = c_o/2$ . The compositions were calculated from the starting stoichiometry.

X-ray diffraction patterns for the compounds with  $x = 0.5$  and  $0.9$  contained split peaks that suggest the presence of two intergrown phases with slightly different lattice constants (Table 3). It is not clear whether the two-phase mixtures resulted from incomplete reaction during high-pressure synthesis or from equilibrium immiscibility at the annealing temperatures and pressures. Nevertheless, the differences between the cell parameters of the two phases (and hence the differences in composition) are sufficiently small that they can be considered as single phases for the purpose of energetic studies. Thus,

**TABLE 3.** Unit-cell dimensions of the stuffed quartz-derivative phases  $\text{Li}_{1-x}\text{Al}_{1-x}\text{Si}_{1+x}\text{O}_4$  (From Xu et al. in review)

x	a (Å)	c (Å)	V (Å <sup>3</sup> )
0	5.2486(1)	5.5976(1)	133.535(5)
0.2	5.2475(1)	5.4825(2)	130.725(8)
0.33	5.2102(1)	5.4551(1)	128.242(4)
0.5	5.1651(1)	5.4571(1)	126.082(7)
	5.1384(4)	5.4589(3)	124.821(13)
avg*	5.1609(1)	5.4574(1)	125.880(8)
0.69	5.0865(1)	5.4451(1)	122.004(4)
0.9	4.9672(2)	5.4187(2)	115.770(9)
	4.9380(3)	5.4123(3)	114.303(13)
avg*	4.9567(2)	5.4164(2)	115.249(10)
1†	4.91239(4)	5.40385(7)	112.933

\*The weighted average is calculated based on molar ratio of the two phases identified at this composition.

†From Will et al. (1988).

weighted average lattice constants were calculated based on molar ratios of two intergrown phases (Table 3). For another high-pressure product with  $x = 0.7$ , diffraction peaks exhibited more complex splittings that suggest five coexisting phases, and we were unable to determine their individual cell dimensions by Rietveld analysis. Instead, a glass-annealed sample with a similar composition ( $x = 0.69$ ) was studied.

As shown in Figures 4a and 4b, the dependence of lattice parameters  $a$  and  $c$  on composition changes character at  $x \approx 0.3$  and  $x \approx 0.65$ . The first change in slope at  $x \approx 0.3$  corresponds to the compositionally driven Al/Si order-disorder transition as revealed by the loss of superlattice reflections for compositions with  $x$  approximately  $\geq 0.3$ . There is no obvious discontinuity in the dependence of  $V$  on  $x$  at  $\sim 0.3$  (Fig. 4c), suggesting a continuous nature to the order-disorder transition.

We interpret the change in slope at  $x \approx 0.65$  as evidence for a transformation from the  $\beta$  to the  $\alpha$  quartz structure. For silica-rich compositions in the series, Li concentrations are too low to prop open the  $\beta$ -quartz structure, and the framework collapses to the denser  $\alpha$ -quartz structure. The displacive transition at  $x \approx 0.65$  is manifested through a change in volume as a function of composition because of the significantly different densities of the  $\alpha$ - and  $\beta$ -quartz frameworks. A detailed crystallographic treatment of the structural changes associated with the two transitions as revealed by in situ synchrotron XRD is presented in a separate paper (Xu et al. in review).

**TABLE 4.** Enthalpies of drop solution and solution in lead borate and heat contents at 974 K of the stuffed quartz-derivative phases  $\text{Li}_{1-x}\text{Al}_{1-x}\text{Si}_{1+x}\text{O}_4$ 

Composition (x)	$\Delta H_{\text{drop-soln},974}$ (kJ/mol)*	$H_{974} - H_{298}$ (kJ/mol)*	$\Delta H_{\text{soln},974}$ (kJ/mol)†
0	153.69 $\pm$ 0.62(6)	104.71 $\pm$ 0.86(6)	48.98 $\pm$ 1.06
0.2	137.98 $\pm$ 1.29(7)	99.96 $\pm$ 1.39(6)	38.02 $\pm$ 1.90
0.25	127.42 $\pm$ 1.11(7)	97.51 $\pm$ 0.68(4)	29.91 $\pm$ 1.30
0.33	116.08 $\pm$ 0.68(4)	93.14 $\pm$ 1.92(4)	22.94 $\pm$ 2.04
0.5	107.33 $\pm$ 1.80(4)	91.00 $\pm$ 0.78(3)	16.33 $\pm$ 1.96
0.69	97.83 $\pm$ 0.68(6)	89.29 $\pm$ 0.84(5)	8.54 $\pm$ 1.08
0.7	96.11 $\pm$ 0.55(4)	89.01 $\pm$ 0.64(3)	7.09 $\pm$ 0.84
0.9	79.94 $\pm$ 1.18(5)	85.14 $\pm$ 1.65(4)	-5.20 $\pm$ 2.03
1	78.2 $\pm$ 0.6‡	87.54 $\pm$ 0.96§	-8.70 $\pm$ 0.24§
			-7.02 $\pm$ 0.36

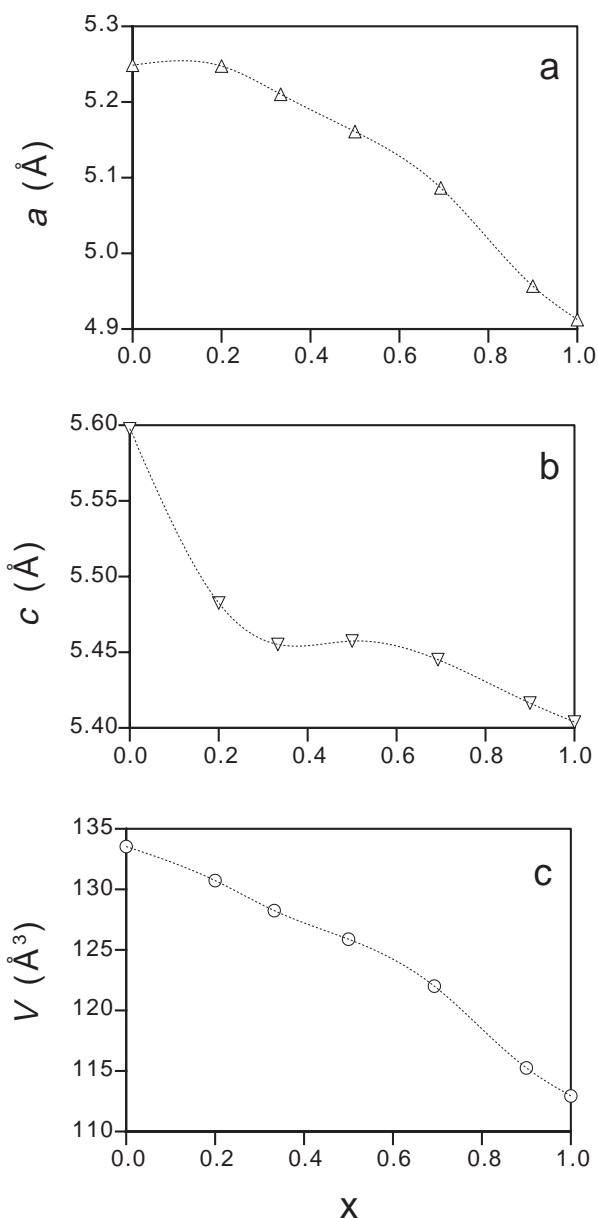
\* Uncertainty is two standard deviations of mean; value in parentheses is the number of experiments.

†  $\Delta H_{\text{soln},974} = \Delta H_{\text{drop-soln},974} - (H_{974} - H_{298})$ .

‡ Average of many measurements done in Navrotsky's laboratory.

§ From Petrovic et al. (1996).

|| From Akaogi and Navrotsky (1984).

**FIGURE 4.** Variation of the unit-cell parameter (a)  $a$ , (b)  $c$ , and (c)  $V$  with composition ( $x$ ) (Xu et al. in review). The cell parameters are plotted in terms of a quartz-like cell.

#### Enthalpies of drop-solution, heat contents, and enthalpies of solution

The heats of drop-solution ( $\Delta H_{\text{drop-soln}}$ ) and solution ( $\Delta H_{\text{soln}}$ ) of the  $\text{Li}_{1-x}\text{Al}_{1-x}\text{Si}_{1+x}\text{O}_4$  solid solutions ( $0 \leq x \leq 1$ ) at 974 K in the lead borate solvent and their heat contents from 298 to 974 K ( $H_{974} - H_{298}$ ) are presented in Table 4. Whereas  $\Delta H_{\text{drop-soln}}$  and  $H_{974} - H_{298}$  are measured values,  $\Delta H_{\text{soln}}$  is computed as  $\Delta H_{\text{soln}} = \Delta H_{\text{drop-soln}} - (H_{974} - H_{298})$ . All the data are based on a four-oxygen mole. Our calculated  $\Delta H_{\text{soln}}$  value for the end-member  $\beta$ -eucryptite is consistent with previous solution calorimetry measurements by Roy and Navrotsky (1984), although they

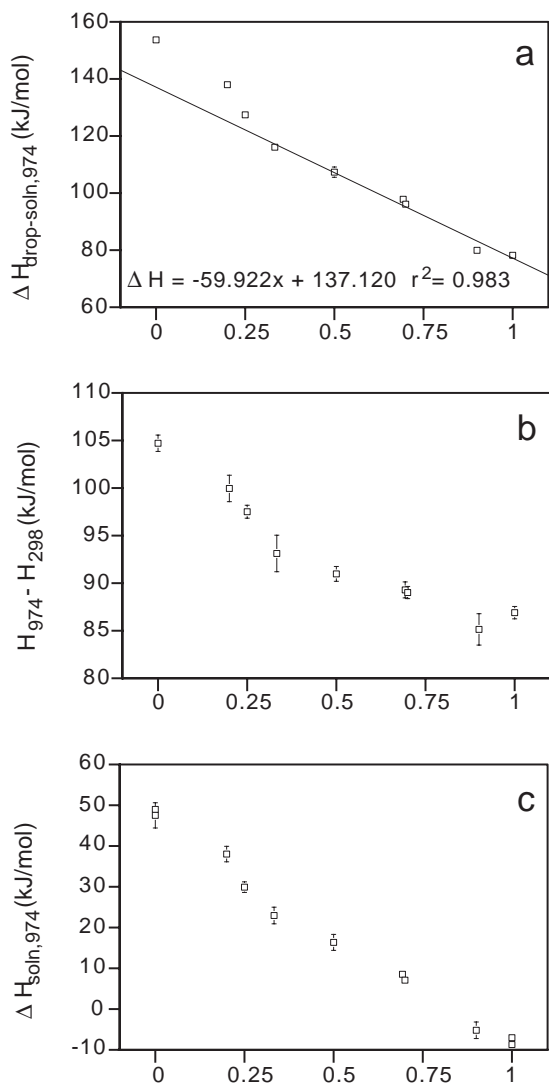


**FIGURE 5.** (a) Enthalpies of drop solution  $\Delta H_{\text{drop-soln},974}$ , (b) heat contents ( $H_{974} - H_{298}$ ), and (c) enthalpies of solution  $\Delta H_{\text{soln},974}$  of the stuffed quartz-derivative phases  $\text{Li}_{1-x}\text{Al}_{1-x}\text{Si}_{1+x}\text{O}_4$  as a function of composition ( $x$ ). The line in **a** represents the  $\Delta H_{\text{drop-soln},974}$  trend for the disordered regime ( $\sim 0.3 \leq x \leq 1$ ).

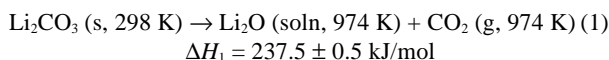
used a sample annealed from glass at 1073 K for 6 days. This agreement implies that their sample and ours contained similar degrees of Al/Si order. Moreover, we note that the enthalpies of two of our samples ( $x = 0.69$  and  $0.7$ ), which were synthesized by different methods (glass-annealing and high-pressure), are in good agreement. Although synchrotron XRD revealed that the sample with  $x = 0.7$  contained five intergrown phases with slightly different lattice constants, the agreement in the measured enthalpies for  $x = 0.69$  and  $x = 0.7$  indicates that these small structural deviations do not exert strong energetic effects. Consequently, we assume that the enthalpy values obtained for the two biphasic samples ( $x = 0.5$  and  $0.9$ ) are representative of the enthalpies of their single phase stoichiometries.

Figure 5 shows  $\Delta H_{\text{drop-soln}}$ ,  $H_{974} - H_{298}$ , and  $\Delta H_{\text{soln}}$  as a function of composition. The behaviors revealed by these three plots are very similar: enthalpies become less endothermic as the sample compositions become more siliceous. This behavior implies an exothermic enthalpy of the charge-coupled substitution  $\text{Si}^{4+} \rightarrow \text{Al}^{3+} + \text{Li}^+$  in these structures, as noted by Roy and Navrotsky (1984). Furthermore, the Al/Si order-disorder transition at  $x \cong 0.3$  is clearly reflected in the enthalpic behavior of the system. The discontinuous increase in enthalpies when  $x$  drops below  $\sim 0.3$  reflects the stabilizing influence of Al/Si ordering in this system. Accordingly, from an energetic perspective the  $\text{LiAlSiO}_4$ - $\text{SiO}_2$  system can be divided into two regimes,  $0 \leq x < \sim 0.3$  and  $\sim 0.3 \leq x \leq 1$ .

### Enthalpies of formation

Using thermodynamic parameters of the constituent oxides ( $\text{Li}_2\text{O}$ ,  $\text{Al}_2\text{O}_3$ , and  $\text{SiO}_2$ ) and the measured calorimetric data, we calculated the standard molar enthalpies of formation of the  $\text{Li}_{1-x}\text{Al}_{1-x}\text{Si}_{1+x}\text{O}_4$  phases from the oxides and the enthalpies of formation from the elements. For these calculations, enthalpies of drop solution and enthalpies of formation of the simple oxides are needed; the values used are listed in Table 5. The  $\Delta H_{\text{drop-soln}}$  of  $\text{Li}_2\text{O}$  is derived from our own drop-solution experiments of  $\text{Li}_2\text{CO}_3$ ; all others are taken from the literature.

**Determination of  $\Delta H_{\text{drop-soln}}$  of  $\text{Li}_2\text{O}$ .** Because  $\text{Li}_2\text{O}$  tends to absorb moisture to form  $\text{LiOH} \cdot \text{H}_2\text{O}$ , it is difficult to determine its  $\Delta H_{\text{drop-soln}}$  directly. Instead, we measured the more stable compound  $\text{Li}_2\text{CO}_3$ . The  $\Delta H_{\text{drop-soln}}$  of  $\text{Li}_2\text{O}$  was calculated from  $\Delta H_{\text{drop-soln}}$  of  $\text{Li}_2\text{CO}_3$  and other related thermochemical parameters. A synthetic lithium carbonate (Aesar, 99.999%) was used and it was dried at 398 K before the calorimetric experiments. The average  $\Delta H_{\text{drop-soln}}$  value for six drops is  $237.5 \pm 0.5$  kJ/mol (Table 6). The thermodynamic cycle used to calculate  $\Delta H_{\text{drop-soln}}$  of  $\text{Li}_2\text{O}$  is:



**TABLE 5.** Enthalpies of drop solution in lead borate at 974 K and enthalpies of formation from elements at 298.15 K of oxides [ $\text{Li}_2\text{O}$ ,  $\alpha$ - $\text{Al}_2\text{O}_3$  (corundum),  $\text{SiO}_2$  (quartz)] used in calculations of the enthalpies of formation in the system

oxides	$\Delta H_{\text{drop-soln},974}$ (kJ/mol)	$\Delta H_f^\circ(298.15 \text{ K})$ (kJ/mol)
$\text{Li}_2\text{O}$	$-18.28 \pm 2.17^*$	$-598.730 \pm 2.1^\ddagger$
$\text{Al}_2\text{O}_3$	$107.9 \pm 1.0^\dagger$	$-1675.692 \pm 1.2^\ddagger$
$\text{SiO}_2$	$39.1 \pm 0.3^\dagger$	$-910.857 \pm 1.7^\ddagger$

\* Derived from our drop solution experiments of  $\text{Li}_2\text{CO}_3$ .

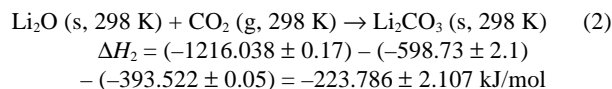
† Average of many measurements done in Navrotsky's laboratory.

‡ Taken from JANAF (Chase et al. 1985).

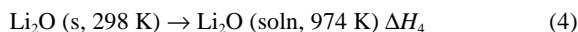
**TABLE 6.** Enthalpy of drop solution of  $\text{Li}_2\text{CO}_3$  in lead borate at 974 K

mass (mg)	$\Delta H_{\text{drop-soln},974}$ (kJ/mol)
16.84	237.482
15.22	238.537
14.78	237.620
15.89	237.750
15.11	236.727
15.70	236.916
avg	$237.5 \pm 0.5^*$

\*Error is 2 standard deviations of mean.

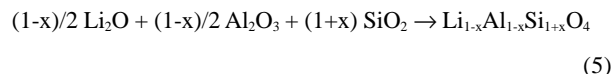


$$\Delta H_3 = -\int_{298}^{974} C_p dT = -31.999 \text{ kJ/mol}$$

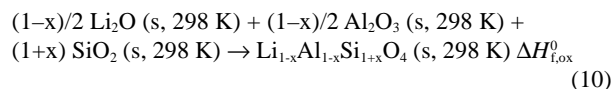
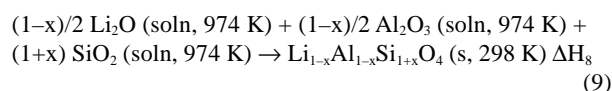
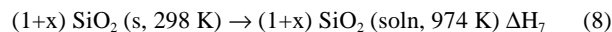
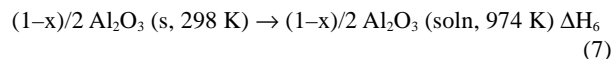
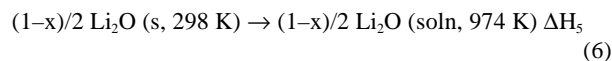


where  $\Delta H_1$  is the measured  $\Delta H_{\text{drop-soln}}$  of  $\text{Li}_2\text{CO}_3$ ;  $\Delta H_2$  is computed from enthalpies of formation of  $\text{Li}_2\text{O}$ ,  $\text{CO}_2$ , and  $\text{Li}_2\text{CO}_3$  (JANAF, Chase et al. 1985); and  $\Delta H_3$  is calculated by integrating  $C_p$  ( $= 88.11 - 2.698 \times 10^{-3}T + 7.233 \times 10^{-5}T^2 - 1.007 \times 10^{-7}T^3$ ) J/mol·K, Robie and Hemingway 1995) from 974 to 298 K. The enthalpy of drop-solution of  $\text{Li}_2\text{O}$ ,  $\Delta H_4$ , therefore, is:  $\Delta H_4 = \Delta H_1 + \Delta H_2 + \Delta H_3 = -18.28 \pm 2.17$  kJ/mol.

**Calculations of  $\Delta H_{\text{f,ox}}^0$  and  $\Delta H_{\text{f,el}}^0$  for the  $\text{Li}_{1-x}\text{Al}_{1-x}\text{Si}_{1+x}\text{O}_4$  phases.** For the reaction involving the formation of the  $\text{Li}_{1-x}\text{Al}_{1-x}\text{Si}_{1+x}\text{O}_4$  stuffed quartz-derivative phases from their constituent oxides at 298 K ( $\Delta H_{\text{f,ox}}^0$ ):



the following thermochemical cycle is used to calculate the standard molar enthalpy of formation:



from which the enthalpies of formation of the stuffed quartz-derivative phases from the oxides are computed according to the formula:  $\Delta H_{\text{f,ox}}^0 = \Delta H_5 + \Delta H_6 + \Delta H_7 + \Delta H_8$ .

**TABLE 7.** Standard molar (per four oxygen mole) enthalpies of formation from elements and oxides, and molar weights of the stuffed quartz-derivative phases  $\text{Li}_{1-x}\text{Al}_{1-x}\text{Si}_{1+x}\text{O}_4$

Composition (x)	Enthalpy of formation (kJ/mol) from		Molar weight
	Elements	Oxides	
0	-2117.84±2.50	-69.78±1.38	126.0056
0.2	-2058.01±2.80	-55.21±1.65	124.8382
0.25	-2036.42±2.74	-44.94±1.47	124.5464
0.33	-2006.69±2.65	-34.07±1.12	124.0600
0.5	-1961.17±3.27	-26.28±1.95	123.0871
0.69	-1909.08±3.04	-17.87±0.93	121.9606
0.7	-1905.81±3.03	-16.19±0.83	121.9197
0.9	-1845.52±3.49	-1.17±1.32	120.7523
1	-1821.71±3.4*	0	120.1686

\*Taken from JANAF (Chase et al. 1985).

Similarly, the enthalpies of formation of the  $\text{Li}_{1-x}\text{Al}_{1-x}\text{Si}_{1+x}\text{O}_4$  phases from the elements ( $\Delta H_{\text{f,el}}^0$ ) can be derived from their values of  $\Delta H_{\text{f,ox}}^0$  and the  $\Delta H_{\text{f,el}}^0$  values of  $\text{Li}_2\text{O}$ ,  $\text{Al}_2\text{O}_3$ , and  $\text{SiO}_2$  by using an appropriate reaction cycle. All the enthalpies of formation thus obtained are summarized in Table 7. With the exceptions of the end-members  $\beta$ -eucryptite and  $\alpha$ -quartz, this work represents the first determination of the enthalpies of formation in this system.

Barany and Adami (1966) measured the heat of solution of  $\beta$ -eucryptite in HF at 346.7 K by solution calorimetry. The  $\Delta H_{\text{f,ox}}^0$  and  $\Delta H_{\text{f,el}}^0$  derived from their  $\Delta H_{\text{soln}}$  value are  $-67.21 \pm 2.76$  and  $-2111.69 \pm 2.2$  kJ/mol, respectively, which are in good agreement with our own values (Table 7). This agreement also demonstrates the consistency of the HF and  $2\text{PbO} \cdot \text{B}_2\text{O}_3$  methods of solution calorimetry.

## DISCUSSION

### Energetics of Al/Si disorder

The disappearance of Al/Si long-range order across the  $\text{LiAlSiO}_4$ - $\text{SiO}_2$  series is consistent with the Al avoidance principle: in framework aluminosilicates, Al-O-Al linkages destabilize the structure and the number of these linkages is minimized (Loewenstein 1954; Goldsmith and Laves 1955). Because of its 1:1 Al to Si ratio, the end-member  $\beta$ -eucryptite has a strong tendency to form a framework in which Al-tetrahedra alternate rigorously with Si-tetrahedra. With increasing silica content, the number of Al-O-Al linkages decreases in the disordered structure and thus the energy difference between the ordered and disordered modifications also decreases.

Enthalpies of solution in the eucryptite-quartz series are compared in Figure 6 with enthalpies obtained for  $\text{Li}_{1-x}\text{Al}_{1-x}\text{Si}_{1+x}\text{O}_4$  glasses by Roy and Navrotsky (1984). With increasing silica content, the difference in  $\Delta H_{\text{soln}}$  decreases from  $x = 0$  to  $x \approx 0.3$ , but the difference remains approximately unchanged thereafter. Thus, the heat of vitrification ( $\Delta H_{\text{vit}}$ ), which

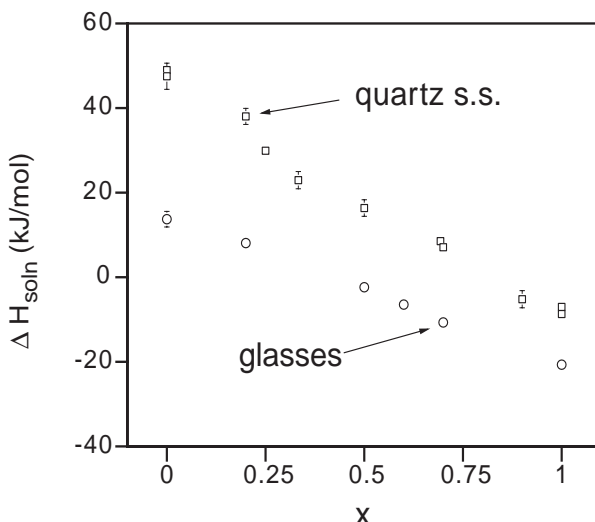


**FIGURE 6.** Enthalpies of solution  $\Delta H_{\text{soln,974}}$  of stuffed quartz-derivative phases and glasses with the composition  $\text{Li}_{1-x}\text{Al}_{1-x}\text{Si}_{1+x}\text{O}_4$  as a function of  $x$ . The data for glasses are from Roy and Navrotsky (1984).

is the enthalpy difference between the crystal and the glass of the same composition, decreases when  $x$  is increased from 0 to  $\sim 0.3$ , yet it is constant for  $\sim 0.3 \leq x \leq 1$ . This behavior may be attributed to the Al/Si distributions in crystal and glass, as the glass probably maintains a relatively random distribution for all compositions, whereas the stuffed quartz-derivative series exhibits two distinct regimes, as described above. In particular, the larger  $\Delta H_{\text{vit}}$  values for the ordered stuffed quartz-derivative phases ( $0 \leq x < \sim 0.3$ ) indicate that these phases are more stable than the disordered phases, and their stability increases with increasing degree of Al/Si order.

**Enthalpy of Al/Si disorder in  $\beta$ -eucryptite.**  $\beta$ -eucryptite polymorphs with a range of Al/Si disorder can be synthesized by annealing glasses with the appropriate end-member composition at different temperatures and times. To determine the enthalpy associated with Al/Si disorder in  $\beta$ -eucryptite, we prepared a suite of  $\beta$ -eucryptite samples by the glass-annealing method and measured the enthalpies of drop-solution. These  $\Delta H_{\text{drop-soln}}$  values (Table 2) ranged from  $138.11 \pm 0.31$  kJ/mol for the most disordered sample (crystallized at 1073 K for 1 h) to  $153.72 \pm 1.93$  kJ/mol for the fully ordered sample (crystallized at 1323 K for 5.25 h).

The difference between these values,  $15.61 \pm 1.95$  kJ/mol, would represent the enthalpy of the order/disorder transition if the distribution of Al and Si atoms in our most-disordered samples were truly random. Recent  $^{29}\text{Si}$  NMR analysis of one of our highly disordered end-members (Phillips et al. in preparation), however, has revealed a significant degree of short-range order; the fraction of Al-O-Al bonds per formula unit ( $N_{\text{Al-Al}}$ ) was close to 0.55, where  $N_{\text{Al-Al}}$  is 0 in a completely ordered structure and 1 in a fully disordered framework. Calculations based on these NMR results and our calorimetric data suggest a revised value for the enthalpy of Al/Si disordering of  $25.9 \pm 2.6$  kJ/mol (Phillips et al. in preparation).

**Critical Al concentrations.** Dove et al. (1996) have explored the role that non-random Al/Si distributions play at the local scale in aluminosilicates of intermediate compositions with long-range Al/Si disorder. For instance, critical disordering temperatures ( $T_c$ ) are dramatically lower in structures that contain less than 1:1 ratios of Al to Si. The disordering  $T_c$  in anorthite ( $\text{CaAl}_2\text{Si}_2\text{O}_8$ ) was estimated to be 2300–2500 K (Carpenter et al. 1990; Carpenter 1992), whereas that in albite ( $\text{NaAlSi}_3\text{O}_8$ ) was calculated by Salje (1990) to occur at 833 K — too low to be measured experimentally. The dramatic discrepancy in critical temperatures arises because Al avoidance can be achieved over short length scales when the fraction of Al in tetrahedral sites ( $f_{\text{Al}}$ ) falls below 0.5. Recent Monte Carlo and statistical mechanical treatments of Al/Si ordering in framework silicates (Myers et al. 1998; Myers 1998; Vinograd and Putnis 1999) allow for Al-O-Al avoidance by local dilution effects. These computer simulations predict that for a variety of aluminosilicate frameworks, critical Al/Si disordering temperatures ( $T_c$ ) fall rather sharply to absolute zero at fractional Al occupancies of 0.29 to 0.34, implying complete long-range disorder for all temperatures when  $f_{\text{Al}}$  falls below these values.

Applying the results of these simulations to the  $\text{Li}_{1-x}\text{Al}_{1-x}\text{Si}_{1+x}\text{O}_4$  system is complicated by several considerations. Most of the stuffed quartz-derivative phases with inter-

mediate compositions do not exhibit stability fields (Fig. 1). Moreover, the phases of intermediate composition ( $x \geq 0.33$ ) in our study were synthesized at pressures of 15–20 kbars and temperatures of 1473–1513 K for very short times (Table 1). Consequently, we cannot assume that the quenched Al/Si distributions in our samples represent equilibrium configurations at those synthesis conditions.

Nevertheless, the predictions of the Monte Carlo models accord with the behavior that we observed in the  $\text{Li}_{1-x}\text{Al}_{1-x}\text{Si}_{1+x}\text{O}_4$  system. Our XRD, TEM, and calorimetry analyses of stuffed quartz-derivative phases all indicate that Al and Si are disordered when  $x$  exceeds  $\sim 0.3$ . This critical composition corresponds to a fractional Al occupancy ( $f_{\text{Al}}$ ) over all tetrahedral sites of  $\sim 0.35$  [with  $f_{\text{Al}} = 1/2(1-x)$ ]. This value is generally consistent with those calculated for aluminosilicate frameworks at elevated temperatures in Myers et al. (1998). We expect that the critical disordering composition for stuffed quartz-derivative phases is similar to that of feldspars ( $T_c = 0$  K at  $f_{\text{Al}} = 0.31$  in Myers et al. 1998), since both structures can be modeled as 2 interpenetrating networks of Al and Si tetrahedra.

On the other hand, the state of Al/Si ordering in our samples is not fully replicated by these Monte Carlo models. First, for purposes of simplicity, Myers et al. elected not to include next-nearest neighbor interactions in their Monte Carlo simulations and, as these authors note, higher-order interactions do contribute to the energetic stabilization produced by Al/Si ordering. Second, their model assumes that complete short-range order prevails in those phases for which  $T_c = 0$  K and  $f_{\text{Al}} \leq 0.31$ .

One of our observations appears more consistent with the possibility that only partial order occurs over short length scales for Al-poor compositions. A value for  $\Delta H_{\text{drop-soln}}$  for disordered  $\beta$ -eucryptite may be determined by extrapolating the enthalpies of those phases within the disordered regime ( $\sim 0.3 \leq x \leq 1.0$ ) to the end-member  $\beta$ -eucryptite composition ( $x = 0$ ) (Fig. 5a); the energy so calculated ( $137.12 \pm 2.76$  kJ/mol) agrees well with the  $\Delta H_{\text{drop-soln}}$  measured directly for our highly disordered  $\beta$ -eucryptite sample ( $139.55 \pm 1.91$  kJ/mol).

In light of the  $^{29}\text{Si}$  NMR results suggesting that this disordered end-member actually is 45% ordered at the local scale (Phillips et al. in preparation), this linear relationship implies a similar degree of short-range order in our specimens for which  $\sim 0.3 \leq x \leq 1.0$ . In other words, all of our Al-poor samples with long-range disorder exhibit nearly even mixtures of order and disorder over short length scales, and the difference in enthalpies between our disordered end-member and the Al-poor samples results almost entirely from the effects of the Li+Al  $\rightarrow$  Si substitution.

### Enthalpy of $\alpha$ - $\beta$ quartz transformation

As described earlier, when only small amounts of Li+Al substitute for Si ( $x$  approximately  $\geq 0.65$ ), the stuffed quartz-derivative phases adopt the  $\alpha$ -quartz structure. At high temperatures, however, these phases transform displacively to the  $\beta$ -quartz-like modifications. The critical temperature ( $T_c$ ) of this transition in pure quartz has been placed at 846 K (e.g., Bachheimer 1980), but  $T_c$  decreases with increasing Li+Al content, as revealed by our own in-situ, high-temperature synchro-

tron XRD data (Xu et al. in review). Since the calorimetric temperature of 974 K places these compounds well into the  $\beta$  stability field, the measured  $\Delta H_{\text{drop-soln}}$  and  $H_{974} - H_{298}$  values actually include the enthalpies associated with the transition ( $\Delta H_{\text{tran}}$ ). Nevertheless, as this displacive transition only involves rotation of Si- or Al-tetrahedra without breakage of Si-O and Al-O bonds,  $\Delta H_{\text{tran}}$  is rather small. For instance, the heat of the  $\alpha$ - $\beta$  quartz transition is only  $1.3 \pm 0.4$  kJ/mol (per four oxygen mole) (Richet et al. 1982), which is of the same order as the error in our calorimetric measurements. Thus, the heat effects associated with the  $\alpha$ - to  $\beta$ -quartz-like transformation in the  $\sim 0.65 \leq x \leq 1$  regime fall within the uncertainties in our calculations. Moreover, unlike the measured enthalpies  $\Delta H_{\text{drop-soln}}$  and  $H_{974} - H_{298}$ , the calculated  $\Delta H_{\text{soln}}$  values represent the heats of solution of the stuffed quartz-derivative phases at 974 K, and hence they correspond to the high-temperature hexagonal structure. These reasons may account for the absence of any transitional features in the dependence of enthalpies on composition for  $x \cong 0.65$ .

### Implications for LAS phase relations

As shown in Table 7, both  $\Delta H_{\text{f,ox}}^0$  and  $\Delta H_{\text{f,el}}^0$  become more endothermic as substitution of Li+Al for Si decreases. In addition, the enthalpies of formation exhibit a change in character at  $x \cong 0.3$  (Fig. 7), which we attribute to the Al/Si order-disorder transition described above. Since  $\Delta H_{\text{f,el}}^0$  includes contributions from constituent oxides, its absolute value is generally much larger than the  $\Delta H_{\text{f,ox}}^0$  of the same composition. As a result, the dependence of  $\Delta H_{\text{f,ox}}^0$  on composition more clearly reveals the order/disorder transition.

A line representing a mechanical mixture between the  $\Delta H_{\text{f,ox}}^0$  data points of the  $\beta$ -eucryptite and  $\alpha$ -quartz end-members is shown in Figure 7. For all compositions between  $x = 0$  and  $x = 1$ , the actual enthalpies of formation are less negative than the enthalpies of the corresponding mechanical mixtures (with the

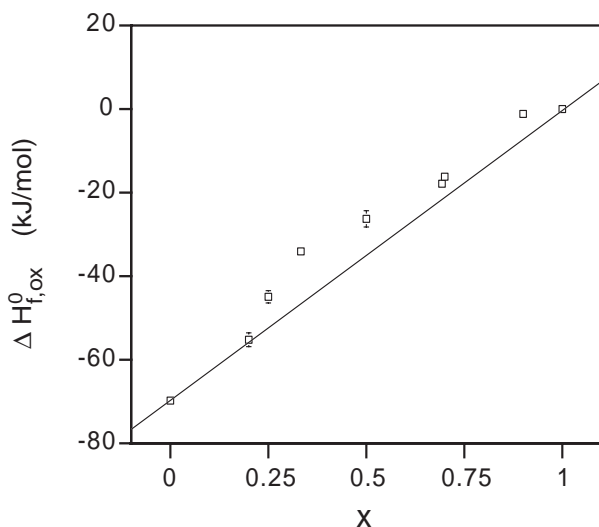


**FIGURE 7.** Standard molar enthalpies of formation of the stuffed quartz-derivative phases  $\text{Li}_{1-x}\text{Al}_x\text{Si}_{1-x}\text{O}_4$  from oxides as  $\alpha$  function of composition ( $x$ ). The line links the data points for the end-members  $\beta$ -eucryptite and  $\alpha$ -quartz.

exception of  $x = 0.2$ ). Therefore, intermediate compositions, particularly those without thermodynamic stability at ambient pressure ( $\sim 0.22 < x < 1$ ), are less stable energetically than the two end-members  $\beta$ -eucryptite and  $\alpha$ -quartz. The lower thermodynamic stability of these intermediate compounds relative to the two end-members is consistent with the postulated phase equilibria in the LAS system (Fig. 1). Whereas  $\beta$ -eucryptite-rich compounds ( $0 < x < \sim 0.22$ ) and quartz persist at high temperatures ( $> 1173$  K), intermediate phases tend either to transform to keatite solid solutions or to decompose into keatite s.s. and  $\alpha$ -cristobalite upon prolonged heating.

Compositions for commercial low CTE (coefficients of thermal expansion) glass-ceramics in the LAS system generally lie within the range of  $x = 0.15$ – $0.44$  due to the appropriate viscosity of their melts, which are used in high-speed glass-forming processes (Beall 1994). Nevertheless, our calorimetric data suggest that  $\beta$ -eucryptite-rich phases ( $0 \leq x < \sim 0.22$ ) are better suited for applications that require superior thermal stability at temperatures higher than 1173 K.

### ACKNOWLEDGMENTS

We are grateful to R.C. Liebermann for useful suggestions regarding the high-pressure synthesis experiments, to G.H. Beall for providing the  $\text{Li}_{0.31}\text{Al}_{0.31}\text{Si}_{0.69}\text{O}_4$  sample, and to B.L. Phillips for providing the unpublished NMR data. We acknowledge constructive reviews of this manuscript by G.L. Hovis, D.C. Palmer, and J.W. Carey. We also thank D.E. Cox, P.M. Woodward, Q. Zhu, and D.M. Yates for help with synchrotron data collection, E.P. Vicenzi for assistance with the microprobe analyses, and J. Linton, D. Dooley, and M. Schoenitz for help with piston-cylinder experiments. This work was supported by the NSF grants EAR-9418031 and EAR-9706143 (to P.J.H.) and the 1996 and 1997 ICDD crystallography scholarships (to H.X.). Some synthesis experiments were performed in the Stony Brook High Pressure Laboratory, which is jointly supported by the State University of New York at Stony Brook and the NSF Science and Technology Center for High Pressure Research (CHiPR) (EAR 89-20239). Synchrotron XRD was carried out at the National Synchrotron Light Source, Brookhaven National Laboratory, which is supported by the U.S. Department of Energy, Division of Material Sciences, and Division of Chemical Sciences. Electron microscopy was conducted at the General Motors Electron Microbeam Facility of the Princeton Materials Institute. Calorimetric experiments were performed in the Princeton Calorimetry Laboratory, supported by CHiPR.

### REFERENCES CITED

- Akaogi, M. and Navrotsky, A. (1984) The quartz-coesite-stishovite transformations: New calorimetric measurements and calculation of phase diagrams. *Physics of the Earth and Planetary Interiors*, 36, 124–134.
- Alpen, U., Schulz, H., Talat, G.H., and Böhm, H. (1977) One-dimensional cooperative Li-diffusion in  $\beta$ -eucryptite. *Solid State Communications*, 23, 911–914.
- Bachheimer, J.P. (1980) An anomaly in the  $\beta$  phase near the  $\alpha$ - $\beta$  transition of quartz. *Journal de Physique-Letters*, 41, L559–L561.
- Barany, R. and Adami, L.H. (1966) Heats of formation of lithium sulfate and five potassium- and lithium-aluminum silicates, 18 p. Bureau of Mines, Washington, D.C.
- Beall, G.H. (1994) Industrial applications of silica. In *Mineralogical Society of America Reviews in Mineralogy*, 29, 469–505.
- Beall, G.H., Karstetter, B.R., and Rittler, H.L. (1967) Crystallization and chemical strengthening of stuffed  $\beta$ -quartz glass-ceramics. *Journal of the American Ceramic Society*, 50, 181–190.
- Buerger, M.J. (1954) The stuffed derivatives of the silica structures. *American Mineralogist*, 39, 600–614.
- Carpenter, M.A. (1991) Mechanisms and kinetics of Al-Si ordering in anorthite: II. Energetics and a Ginzburg-Landau rate law. *American Mineralogist*, 76, 1120–1133.
- Carpenter, M.A. (1992) Equilibrium thermodynamics of Al/Si ordering in anorthite. *Physics and Chemistry of Minerals*, 19, 1–24.
- Carpenter, M.A., Putnis, A., Navrotsky, A., and McConnell, D.C. (1983) Enthalpy effects associated with Al/Si ordering in anhydrous Mg-cordierite. *Geochimica et Cosmochimica Acta*, 47, 899–906.
- Carpenter, M.A., McConnell, D.C., and Navrotsky, A. (1985) Enthalpies of Al/Si ordering in the plagioclase feldspar solid solution. *Geochimica et Cosmochimica Acta*, 49, 947–966.

- Carpenter, M.A., Angel, R.J., and Finger, L.W. (1990) Calibrations of Al/Si order variations in anorthite. *Contributions to Mineralogy and Petrology*, 104, 471–480.
- Chase, M.W. Jr., Davies, C.A., Downey, J.R. Jr., Frurip, D.J., McDonald, R.A., and Syverud, A.N. (1985) JANAF Thermochemical Tables (3rd edition). *Journal of Physical and Chemical Reference Data*, Vol. 14, Supplement, 1.
- Cox, D.E., Toby, B.H., and Eddy, M.M. (1988) Acquisition of powder diffraction data with synchrotron radiation. *Australian Journal of Physics*, 41, 117–131.
- Dove, M.T., Thayaparam, S., Heine, V., and Hammonds, K.D. (1996) The phenomenon of low Al-Si ordering temperatures in aluminosilicate framework structures. *American Mineralogist*, 81, 349–362.
- Goldsmith, J.R. and Laves, F. (1955) Cation order in anorthite ( $\text{CaAl}_2\text{Si}_2\text{O}_8$ ) as revealed by gallium and germanium substitutions. *Zeitschrift für Kristallographie*, 106, 213–226.
- Guth, H. and Heger, G. (1979) Temperature dependence of the crystal structure of the one-dimensional  $\text{Li}^+$ -conductor  $\beta$ -eucryptite ( $\text{LiAlSi}_4\text{O}_{10}$ ). In P. Vashista, J.N. Mundy, and G.K. Shenoy, Eds., *Fast ion transport in solids*, p. 499–502. Elsevier, North Holland, New York.
- Hatch, R.A. (1943) Phase equilibrium in the system  $\text{Li}_2\text{O}-\text{Al}_2\text{O}_3-\text{SiO}_2$ . *American Mineralogist*, 28, 471–496.
- Heaney, P.J. and Veblen, D.R. (1991) Observations of the  $\alpha$ - $\beta$  phase transition in quartz: A review of imaging and diffraction studies and some new results. *American Mineralogist*, 76, 1018–1032.
- Hovis, G.L. and Navrotsky, A. (1995) Enthalpies of mixing for disordered alkali feldspars at high temperature: A test of regular thermodynamic models and a comparison of hydrofluoric acid and lead borate solution calorimetric techniques. *American Mineralogist*, 80, 280–284.
- Hummel, F.A. (1952) Significant aspects of certain ternary compounds and solid solutions. *Journal of the American Ceramic Society*, 35, 64–66.
- Larson, A.C. and Von Dreele, R.B. (1994) GSAS, General Structure Analysis System. Los Alamos National Laboratory, New Mexico, 179 p.
- Lichtenstein, A.I., Jones, R.O., Xu, H., and Heaney, P.J. (1998) Anisotropic thermal expansion in the silicate  $\beta$ -eucryptite: A neutron diffraction and density functional study. *Physical Review B* 58, 6219–6223.
- Loewenstein, W. (1954) The distribution of aluminum in the tetrahedra of silicates and aluminates. *American Mineralogist*, 39, 92–96.
- Li, C.T. (1968) The crystal structure of  $\text{LiAlSi}_4\text{O}_{10}$  III (high-quartz solid solution). *Zeitschrift für Kristallographie*, 127, 327–348.
- Müller, W.F. and Schulz, H. (1976) Antiphase domains in  $\beta$ -eucryptite ( $\text{LiAlSi}_4\text{O}_{10}$ ). *Naturwissenschaften*, 63, 294.
- Munoz, J.L. (1969). Stability relations of  $\text{LiAlSi}_2\text{O}_6$  at high pressures. *Mineralogical Society of America Special Paper*, 2, 203–209.
- Myers, E.R. (1998) A statistical-mechanics model of ordering in aluminosilicate solid solutions. *Physics and Chemistry of Minerals*, 25, 465–468.
- Myers, E.R., Heine, V., and Dove, M.T. (1998) Thermodynamics of Al/Al avoidance in the ordering of Al/Si tetrahedral framework structures. *Physics and Chemistry of Minerals*, 25, 457–464.
- Nagel, W. and Böhm, H. (1982) Ionic conductivity studies on  $\text{LiAlSi}_4\text{O}_{10}$ - $\text{SiO}_2$  solid solutions of the high quartz type. *Solid State Communications*, 42, 625–631.
- Navrotsky, A. (1997) Progress and new directions in high temperature calorimetry revisited. *Physics and Chemistry of Minerals*, 24, 222–241.
- Navrotsky, A., Rapp, R.P., Smelik, E., Bumly, P., Circone, S., Chai, L., Bose, K., and Westrich, H.R. (1994) The behavior of water and carbon dioxide in high temperature lead borate solution calorimetry of volatile-bearing phases. *American Mineralogist*, 79, 1099–1109.
- Palmer, D.C. (1994) Stuffed derivatives of the silica polymorphs. In *Mineralogical Society of America Reviews in Mineralogy*, 29, 83–122.
- Petrovic, I., Heaney, P.J., and Navrotsky, A. (1996) Thermochemistry of the new silica polymorph moganite. *Physics and Chemistry of Minerals*, 23, 119–126.
- Pillars, W.W. and Peacor D.R. (1973) The crystal structure of beta eucryptite as a function of temperature. *American Mineralogist*, 58, 681–690.
- Ribbe, P.H. (1983) Aluminum-silicon order in feldspars: Domain textures and diffraction patterns. In *Mineralogical Society of America Reviews in Mineralogy*, 2, 21–55.
- Richert, P., Bottinga, Y., Denielon, L., Petit, J.P., and Tequi, C. (1982) Thermodynamic properties of quartz, cristobalite and amorphous  $\text{SiO}_2$ : Drop calorimetry measurements between 1000 and 1800 K and a review from 0 to 2000 K. *Geochimica et Cosmochimica Acta*, 46, 2639–2658.
- Robie, R.A. and Hemingway, B.S. (1995) Thermodynamic properties of minerals and related substances at 298.15 K and 1 bar (105 Pascals) pressure and at higher temperatures. U.S. Geological Survey Bulletin 2131, Washington, D.C.
- Roy, B.N. and Navrotsky, A. (1984) Thermochemistry of charge-coupled substitutions in silicate glasses: The systems  $\text{M}_{1/n}\text{AlO}_2\text{-SiO}_2$  (M = Li, Na, K, Rb, Cs, Mg, Ca, Sr, Ba, Pb). *Journal of the American Ceramic Society*, 67, 606–610.
- Roy, R. and Osborn, E.F. (1949) The system lithium metasilicate-spodumene-silica. *Journal of the American Chemical Society*, 71, 2086–2095.
- Roy, R., Roy, D., and Osborn, E.F. (1950) Compositional and stability relationships among the lithium aluminosilicates: eucryptite, spodumene, and petalite. *Journal of the American Ceramic Society*, 33, 152–159.
- Salje, E.K.H. (1990) Phase transitions in ferroelastic and co-elastic crystals, 366 p. Cambridge University Press, Cambridge.
- Schulz, H. and Tscherry, V. (1972a) Structural relations between the low- and high-temperature forms of  $\beta$ -eucryptite ( $\text{LiAlSi}_4\text{O}_{10}$ ) and low and high quartz. I. Low-temperature form of  $\beta$ -eucryptite and low quartz. *Acta Crystallographica*, B28, 2168–2173.
- (1972b) Structural relations between the low- and high-temperature forms of  $\beta$ -eucryptite ( $\text{LiAlSi}_4\text{O}_{10}$ ) and low and high quartz. II. High-temperature form of  $\beta$ -eucryptite and high quartz. *Acta Crystallographica*, B28, 2174–2177.
- Strnad, Z. (1986) Glass-ceramic materials. *Glass Science and Technology*, Vol. 8. Elsevier, Amsterdam.
- Thompson, P., Cox, D.E., and Hastings, J. (1987) Rietveld refinement of Debye-Scherrer synchrotron X-ray data for  $\text{Al}_2\text{O}_3$ . *Journal of Applied Crystallography*, 20, 79–83.
- Tscherry, V., Schulz, H., and Laves, F. (1972a) Average and super structure of  $\beta$ -eucryptite ( $\text{LiAlSi}_4\text{O}_{10}$ ), Part I, Average structure. *Zeitschrift für Kristallographie*, 135, 161–174.
- (1972b) Average and super structure of  $\beta$ -eucryptite ( $\text{LiAlSi}_4\text{O}_{10}$ ), Part II, Superstructure. *Zeitschrift für Kristallographie*, 135, 175–198.
- Vinograd, V.L. and Putnis, A. (1999) The description of Al, Si ordering in aluminosilicates using the cluster variation method. *American Mineralogist*, 84, 311–324.
- Will, G., Bellotto, M., Parrish, W., and Hart, M. (1988) Crystal structures of quartz and magnesium germanate by profile analysis of synchrotron-radiation high resolution powder data. *Journal of Applied Crystallography*, 21, 182–191.
- Winkler, H.G.F. (1948) Synthese und Kristallstruktur des Eukryptits,  $\text{LiAlSi}_4\text{O}_{10}$ . *Acta Crystallographica*, 1, 27–34.
- Xu, H., Heaney, P.J., and Böhm, H. (1999a) Structural modulations and phase transitions in  $\beta$ -eucryptite: An in-situ TEM study. *Physics and Chemistry of Minerals* (in press).
- Xu, H., Heaney, P.J., Yates, D.M., Von Dreele, R.B., and Bourke, M.A. (1999b) Structural mechanisms underlying near-zero thermal expansion in  $\beta$ -eucryptite: A combined synchrotron x-ray and neutron Rietveld analysis. *Journal of Materials Research* (in press).

MANUSCRIPT RECEIVED NOVEMBER 16, 1998

MANUSCRIPT ACCEPTED MAY 13, 1999

PAPER HANDLED BY J. WILLIAM CAREY